

1 Injury tolerances for oblique impact helmet 2 testing

3 M Aare, S Kleiven and P Halldin

4 *Division of Neuronic Engineering, CTV – Centre for Technology within Healthcare,*
5 *Royal Institute of Technology (KTH) and Karolinska Institute, Stockholm, Sweden.*

6 **Abstract:** The most frequently sustained severe injuries in motorcycle crashes are injuries to the
7 head, and many of these are caused by rotational force. Rotational force is most commonly the result
8 of oblique impacts to the head. Good testing methods for evaluating the effects of such impacts are
9 currently lacking. There is also a need for improving our understanding of the effects of oblique
10 impacts on the human head. Helmet standards currently in use today do not measure rotational
11 effects in test dummy heads. However rotational force to the head results in large shear strains arising
12 in the brain, which has been proposed as a cause of traumatic brain injuries like diffuse axonal
13 injuries (DAI).

14 This paper investigates a number of well-defined impacts, simulated using a detailed finite element
15 (FE) model of the human head, an FE model of the Hybrid III dummy head and an FE model of a
16 helmet. The same simulations were performed on both the FE human head model and the FE Hybrid
17 III head model, both fitted with helmets. Simulations on both these heads were performed to describe
18 the relationship between load levels in the FE Hybrid III head model and strains in the brain tissue
19 in the FE human head model. In this study, the change in rotational velocity and the head injury
20 criterion (HIC) value were chosen as appropriate measurements. It was concluded that both rotational
21 and translational effects are important when predicting the strain levels in the human brain.

22 **Keywords:** Injury tolerances, Oblique impacts, Helmet, Head injuries and FE (Finite Element)

23 INTRODUCTION

24 Motorcycle riders are very exposed in traffic accidents
25 since their level of protection is limited. One way to provide
26 better safety for motorcycle riders is to improve the helmets.
27 The most frequently sustained severe injuries in motorcycle
28 crashes are namely injuries to the head [1]. Many of these
29 injuries are caused by rotational forces [2] that are most
30 commonly generated as a result of oblique impacts found
31 in motorcycle crashes [3]. The most frequent impact is an
32 impact close to the visor attachment points with an average
33 impact thereof speed of 44 km/h and an average angle of
34 28° to the impacted object [3].

35 Most safety helmets are designed to meet the
36 requirements established by standardised tests (e.g.
37 ECE22.05 [4], FMVSS218 [5], and BS6658 [6]). In these
38 tests, the helmet is typically dropped vertically onto a flat
39 or curved rigid surface that is set up for a tangential impact

to the helmet surface. During the drop tests, the 40
translational acceleration of a head form is measured. The 41
British Standard BS6658 includes an oblique impact, but 42
there is no measurement of the rotational effects, which 43
makes it difficult to correlate these effects to injuries in 44
the human brain. The oblique impact tests in the BS 45
6658 ensure: 46

- that projecting visor mounts and other projections shear 47
off easily when there is an impact with a series of parallel 48
bars; and 49
- that the tangential force on the helmet shell, when it 50
impacts with a rough flat surface, is no larger than that 51
of typical shell materials used in 1985 (the year of 52
introduction of the test). 53
54

The ECE22.05 standard also includes a test that can be 55
seen as an oblique impact test. However, this is a test for 56
projection and surface friction, and does not include 57
rotational measurements in the dummy head. Today's 58
standards have resulted in helmets with a good degree of 59
protection for radial impacts while their protection for 60
oblique impacts remains unknown. 61

In an oblique impact to a helmeted head, the rotational 62
energy can be absorbed by (a) frictional energy between 63

Corresponding Author:

M Aare, S Kleiven and P Halldin
Marinens v. 30, 13640 Haninge, Sweden
Tel: +46-704953602
Email: aare@kth.se

64 the helmet shell and the impacting surface, (b) internal
 65 energy in the liner and comfort foam due to shear
 66 deformation, and (c) frictional energy between the liner
 67 and the head.

68 The standard test procedures are based on vary vague
 69 reasons. More realistic would be to test helmets for impacts
 70 similar to the most commonly observed impacts in real
 71 life motorcycle accidents. Aare and Halldin (2003) [7]
 72 proposed a new method to test helmets for oblique impacts,
 73 but they did not propose any injury tolerances for such a
 74 test. The injury tolerances and criteria used when testing
 75 oblique impacts to helmets should predict injuries
 76 frequently seen in traffic accidents. The most frequently
 77 sustained brain injuries in motor vehicle accidents that
 78 result in either fatality or the need for long-term
 79 rehabilitation are subdural hematomas (SDH) and diffuse
 80 axonal injuries (DAI) [2]. The main causes of SDH are
 81 ruptured arteries or bridging veins. DAI is caused by the
 82 tearing of neuronal axons in the brain tissue. It has been
 83 proposed that there are correlations between these injuries
 84 and rotational effects to the head [2]; [8]. In these studies
 85 injury thresholds for purely angular motions was proposed.
 86 If an angular motion is combined with a translational
 87 motion, these thresholds probably have to be decreased,
 88 as shown in the study by DiMasi et al. (1995) [9] and
 89 Ueno and Melvin (1995) [10].

90 To establish tolerances or criteria for an oblique impact
 91 to the helmeted head it is possible to use a detailed finite
 92 element (FE) model of the human head [11]. This method
 93 should be seen as a complement to biological experiments
 94 on human cadavers. It has been suggested that there is a
 95 correlation between the strain in the brain and DAI [12];
 96 [13]. If the FE model of the human head is well correlated
 97 with relevant experiments, then the strain computed in
 98 the model can be compared with accepted tissue-based
 99 injury thresholds. Bain and Meaney (2000) [12] proposed
 100 a threshold of 20% strain in the brain tissue for the onset
 101 of the malfunction of the nerves in the brain, which could
 102 be seen as a first stage of DAI.

103 Currently there is a lack of good testing methods for
 104 evaluating the effects of oblique impacts. There is also a
 105 need for improved understanding of the effects on the
 106 human head subjected to oblique impacts. In current helmet
 107 standards, no rotational effects are measured in the head

108 form, partly because there are no accepted global injury
 109 thresholds for a combination of rotations and translations.
 110 The objective of this study was therefore to study if, and
 111 how, rotational and translational parameters influence the
 112 strain levels in the brain for three well-defined and
 113 commonly observed [3] oblique impacts to helmets.

114 The aim of this study was to propose new injury
 115 tolerances for a specific set of oblique helmet impacts.
 116 Further it was hypothesized that it is possible to predict
 117 the strain in brain tissue using the peak change of rotational
 118 velocity and the HIC value.

METHODS

119 This is a numerical study using the non-linear and dynamic
 120 finite element (FE) code LS-DYNA [14]. In this study,
 121 FE models of (1) the human head [15], (2) a Hybrid III
 122 dummy head [16], and (3) an experimental helmet were
 123 used. Simulations where performed on both the human
 124 head and on the Hybrid III dummy head, wearing the
 125 helmet.
 126

Injury tolerances

127 The maximal principal strain in the brain tissue was chosen
 128 as a predictor of injuries, as it has been shown to correlate
 129 with DAI [12]. A strain of 20% was shown to be critical
 130 to the brain tissue. As the strains in the brain tissue are
 131 proportional to the HIC value for pure translations, and
 132 also proportional to the change in rotational velocity for
 133 pure rotations of short impact durations [11], it is suggested
 134 that the output data is fitted to the following formula:
 135

$$\epsilon = k_1\Delta\omega + k_2HIC \quad [1]$$

136 where ϵ is the maximum strain in the brain tissue, $\Delta\omega$ is
 137 the peak resultant change in rotational velocity, HIC is
 138 the head injury criteria [17] and k_1 and k_2 are constants.
 139 The strain (ϵ) is taken from the FE human head model,
 140 whereas $\Delta\omega$ and HIC are taken from FE Hybrid III head
 141 model.

FE model of the human head

142 The FE model of the human head (Figure 1) developed
 143 at the Royal Institute of Technology (KTH) Stockholm,
 144 Sweden, is based on data from the Visual Human Database
 145

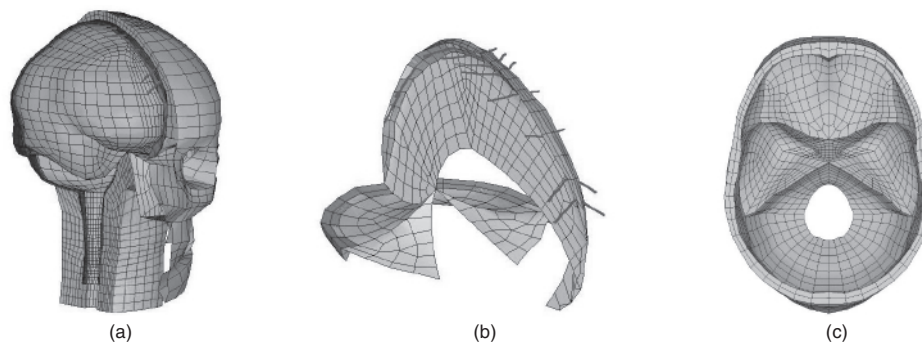


Figure 1 Finite element mesh of (a) the human head, (b) falx and tentorium including transverse and superior sagittal sinuses with bridging veins, and (c) cranium.

146 [18]. The FE model is anatomically detailed and includes
 147 the scalp, the skull, the brain, the meninges, the
 148 cerebrospinal fluid (CSF) and eleven pairs of parasagittal
 149 bridging veins [15], [19], [20] and [21].

150 FE model of the Hybrid III dummy head

151 The FE model of the Hybrid III dummy head is very
 152 similar to the real Hybrid III dummy, with respect to
 153 geometry, mass, inertia, and material properties [16]. The
 154 model used in this study does not include the neck. This
 155 is a simplification used in all standard helmet tests. The
 156 solid part of the head (the aluminium) was modelled as
 157 rigid, whereas the rubber skin was modelled using a
 158 viscoelastic material model [16]. The Hybrid III head model
 159 used in this study was meshed using 2311 elements (two
 160 elements through the thickness in the solid part making a
 161 total of 1288 elements and two elements through the
 162 thickness in the rubber skin making a total of 1023
 163 elements).

164 FE model of the helmet

165 The FE model of the helmet includes a linearly-elastic
 166 material model of the ABS thermoplastic shell, validated
 167 against quasi-static tensile tests (thickness: 4.7 mm, Young's
 168 modulus: 1.64 GPa, density: 1161 kg/m³ and Poisson's
 169 ratio: 0.45). The energy absorbing liner material consists
 170 of expanded polystyrene (EPS) with a density of 40 kg/
 171 m³ modelled using a crushable foam material [14]. This
 172 foam material model requires a stress-strain curve.
 173 Therefore hydrostatic compressive tests were performed
 174 on expanded polystyrene (Figure 2). The data from this
 175 test were implemented in the material model. Poisson's
 176 ratio was estimated to zero and Young's modulus
 177 implemented in the material model was estimated to 8
 178 MPa. Young's modulus implemented in this material model
 179 represents the stiffness during unloading. The stiffness
 180 during loading is taken from the implemented load-curve.
 181 The tensile stress cut-off was estimated at 1 MPa and the
 182 damping coefficient estimated at 0.05 since the material
 183 was assumed not to be strain-rate dependent [22].

184 The helmet model was not fitted with a chinstrap, as it
 185 was concluded when studying high-speed movies from

experiments performed by Aare M. and Halldin P [7] 186
 that the inclusion of a chin strap made no significant 187
 difference to well-fitting helmets during short duration 188
 impacts. 189

The contact definition between (a) the FE model of 190
 the human head and the helmet and (b) the FE model of 191
 the Hybrid III dummy head and the helmet was the 192
 "surface-to-surface interference" [14]. This means that 193
 when the head is larger than the space inside the helmet, 194
 an initial pressure or contact force arises. When the head 195
 is smaller than the space inside the helmet, there is no 196
 initial pressure. However, the inside surface of the helmet 197
 fitted with the Hybrid III head model was shaped to fit 198
 the geometry of the head perfectly. The inside surface of 199
 the helmet fitted with the human head model was shaped 200
 to fit the geometry of that head perfectly. This means that 201
 there was no initial gap between the heads and the helmets 202
 anywhere throughout the contact surfaces. This also means 203
 that the geometry of the inside surface if the helmets 204
 were slightly different. However, the thickness of the liner 205
 in the two different helmets was similar. 206

**FE model of the helmet and the Hybrid III head 207
 combined 208**

The complete model of the helmet and the Hybrid III 209
 dummy was validated against both radial and oblique impact 210
 tests on helmets (Figure 3). Some of these experimental 211
 data was presented by Aare and Halldin (2003) [7]. 212

Numerical simulations 213

Three different impacts were tested, where impact 1 is 214
 to the top of the head inducing sagittal plane rotation, 215
 Impact 2 is lateral inducing axial rotation, and Impact 3 is 216
 lateral inducing coronal plane rotation (Figure 3). For 217
 Impacts 1 and 3, three different impact velocities were 218
 used (5, 7 and 9 m/s), and for Impact 2 an additional 219
 impact velocity of 3 m/s was also used in the testing. 220
 The reason for simulating impact 2 at 3 m/s was that all 221
 the other impact velocities caused strains in the brain 222
 tissue larger than 20%. The impact angles were induced 223
 by altering the speed of the head and the speed of the 224
 impactor (Table 1). For all three impacts and impact 225
 velocities, four different impact angles between the head 226
 and the impactor were tested (30°, 45°, 60° and 90°). 227
 These specific scenarios were chosen to cover the range 228
 of the most commonly observed impacts in real life 229
 motorcycle accidents [3]. 230

Data from the helmeted Hybrid III head was correlated 231
 to load levels in the human brain, by performing simulations 232
 on both the FE human head and the FE Hybrid III head. 233
 Comparisons were made between the strains in the brain 234
 tissue of the FE human head and the change of rotational 235
 velocity and the HIC-value in the FE Hybrid III head for 236
 identical impacts. These comparisons were done to find 237
 the relationship between the global kinematics of a Hybrid 238
 III head and the strains in the human brain. 239

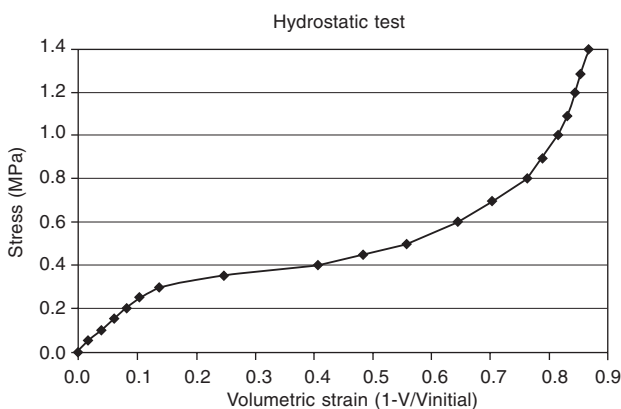


Figure 2 Stress-strain curve from the hydrostatic test.

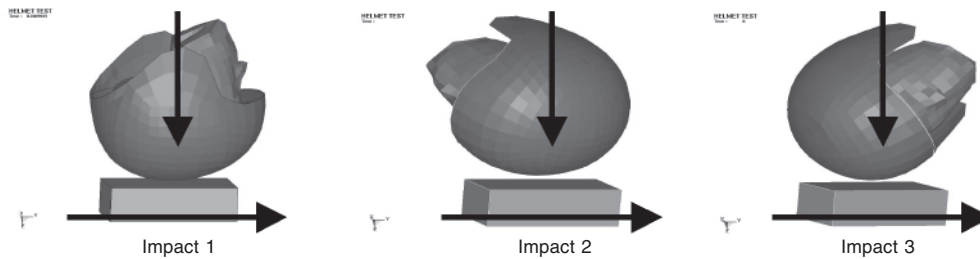


Figure 3 The three different impacts in the numerical simulations.

Table 1 Vertical and horizontal velocities of the different impact speeds and angles used in the numerical simulations.

Angle of impact	Impact velocity: 3 m/s		Impact velocity: 5 m/s		Impact velocity: 7 m/s		Impact velocity: 9 m/s	
	Vertical impact speed (m/s)	Horizontal speed of the plate (m/s)	Vertical impact speed (m/s)	Horizontal speed of the plate (m/s)	Vertical impact speed (m/s)	Horizontal speed of the plate (m/s)	Vertical impact speed (m/s)	Horizontal speed of the plate (m/s)
30°	1.50	2.60	2.50	4.33	3.50	6.06	4.50	7.79
45°	2.12	2.12	3.54	3.54	4.95	4.95	6.36	6.36
60°	2.60	1.50	4.33	2.50	6.06	3.50	7.79	4.50
90°	3.00	0.00	5.00	0.00	7.00	0.00	9.00	0.00

240 **RESULTS**

241 Figure 4 shows a comparison between experiments and
 242 the numerical simulations from impact 1, velocity 7 m/s
 243 and impact angle 45°.

244 The results from the numerical simulations are
 245 presented in Table 2.

246 Comparing the results from the various different
 247 impacts, it is quite clear that the rotational effects have a
 248 major influence on the strain levels in the human brain
 249 (Figures 5, 6 and 7). Each point in these figures represents
 250 one simulated impact. These points were plotted to give
 251 the reader a better picture of which impact scenarios that
 252 are critical. The maximum strain in the brain was usually
 253 found in the white brain tissue, though in different
 254 elements. The constants k_1 and k_2 in Equation 1 were
 255 computed for Impacts 1, 2 and 3 respectively, using least
 256 square regression analyses of Equation 1 (Table 3). The
 257 regression coefficient is a figure that describes how well
 258 the data correlates to the equation. A regression coefficient
 259 of one represents a perfect match and a regression
 260 coefficient of zero represents no correlation at all.

261 Different isostrain curves can be plotted using the
 262 computed constants k_1 and k_2 in Equation 1 (Figures 5, 6
 263 and 7).

264 **DISCUSSION**

265 This study has presented a method for computing test-
 266 specific injury tolerances using an FE model of the human
 267 head. The two regression parameters, HIC and change in
 268 rotational velocity, vary in their influence on the head
 269 response depending on the impact location and orientation
 270 of the helmeted head (Figures 5, 6 and 7). In Impact 1,

the change in rotational velocity exhibits a fairly sharp
 cut-off point for determining safe and unsafe conditions,
 whereas in Impact 2 and 3, the HIC value (or at least a
 translational component) also needs to be considered when
 predicting injury. It is therefore difficult to use the one
 injury tolerance indicator for all types of impacts. It is
 suggested that one specific set of constants be used for
 each impact direction and speed.

Regression analysis was used in this study to fit the
 data to equation 1. The regression coefficient is a figure
 that describes how well the data correlates to the equation.
 A regression coefficient of one represents a perfect match
 and a regression coefficient of zero represents no correlation
 at all. The regression analysis showed good correlations
 for Impacts 1 and 2 (Table 2). For this impact, a formula
 of higher order would probably fit the data better, especially
 for very low changes in rotational velocity. It is likely that
 the curves plotted in figures 5, 6 and 7 are more accurate
 in the central parts of the diagrams close to the load levels
 that are used in the simulations.

The simulated impacts in this study were not only
 chosen to cover the most commonly observed impacts in
 motorcycle accidents, but also to cover rotations around
 all three Cartesian axes. Impact 2 was according to statistics,
 the most common impact in real-life accidents.

The head is vulnerable to accelerations in the lateral
 direction [23], [24] and therefore the HIC values are more
 critical for Impacts 2 and 3 than for Impact 1.

Even when the head was dropped vertically (90°),
 rotations were induced in all the impacts and in particular
 in Impacts 2 and 3. These rotations occur because the
 impact point is not situated directly under the centre of
 gravity.

For rotational impulses of short duration, the change

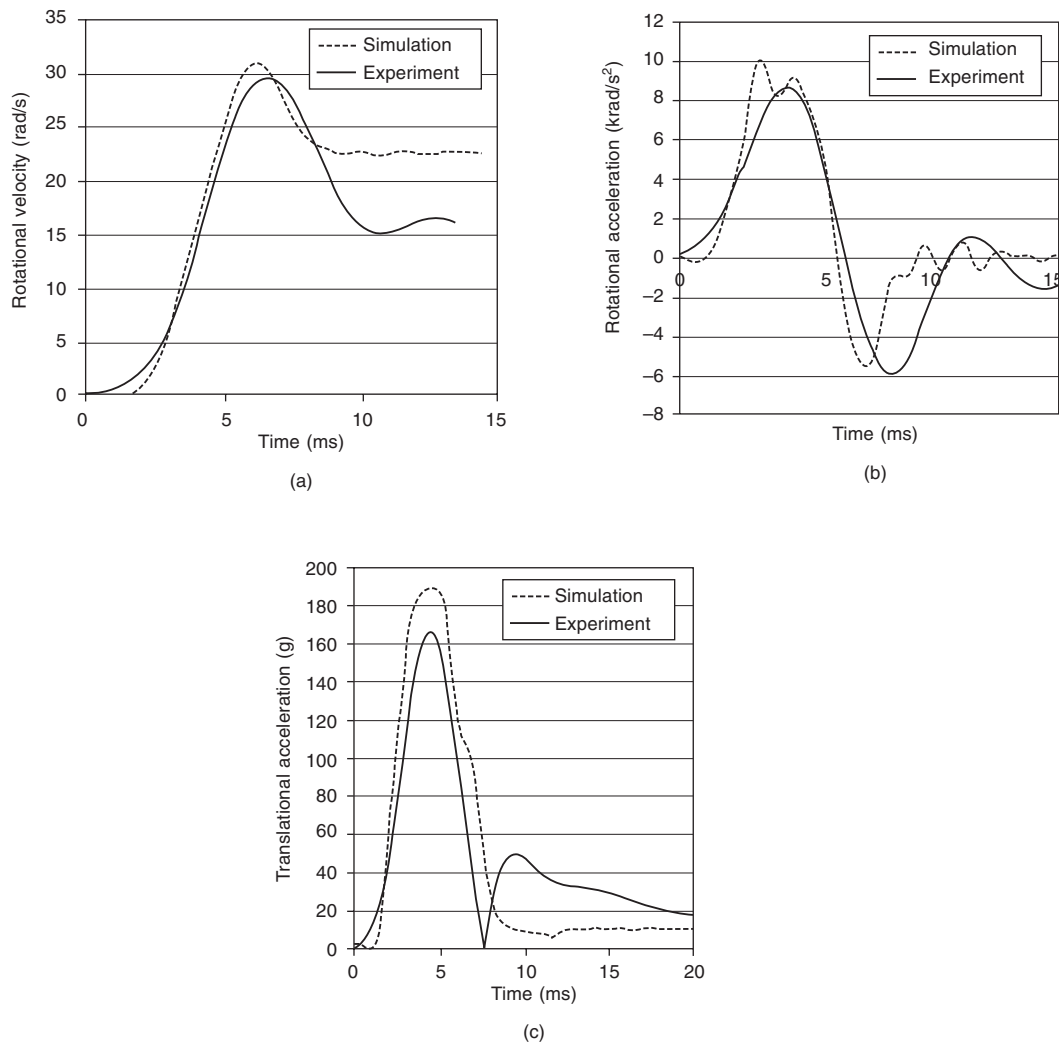


Figure 4 Comparison of simulations and experiments from impact 1 (Figure 3), velocity 7 m/s and impact angle 45°, where (a) is the change of rotational velocity, (b) is rotational acceleration, and (c) is translational acceleration.

305 in angular velocity has been shown to correspond better
 306 than all other parameters with the intracranial strains found
 307 in the FE model [11]. This is in agreement with Holbourn's
 308 hypothesis [13]. For translational impulses on the other
 309 hand, the HIC [17] and the HIP [25] have shown the best
 310 correlation with the strain levels found in the model [11].

311 In Table 2 all data needed to plot Figures 5, 6 and 7 are
 312 displayed. Additionally, the rotational accelerations are
 313 displayed in Table 2, since these parameters are used in
 314 some other injury criteria [8] and might therefore be
 315 interesting to some readers. The translational acceleration
 316 is also displayed in Table 2, since this parameter is correlated
 317 to the HIC-value and might therefore also be of interest.

318 An FE model of the human head was used to compute
 319 the maximal principal strain in the brain, and thereby
 320 analyse the risk for DAI. There are also other tissue-level
 321 measurements that may be used as injury predictors, such
 322 as strain rate, the product of strain and strain rate, von-
 323 Mises stress, and strain energy. In this study, the strain
 324 has been chosen to analyse the risk for DAI, as this
 325 measurement has been experimentally verified previously

[12], [26]. An FE model needs to be well correlated to 326
 relevant experimental studies on the human brain. Another 327
 important issue in modelling of the human head is the 328
 selection of appropriate material properties for various 329
 intracranial structures. The choice of shear properties for 330
 the brain tissue is difficult as the range of published values 331
 varies several orders of magnitude [21]; [27]. However, 332
 FE model used in this study has been carefully validated 333
 and shown to have a good correlation with experiments 334
 found in the literature including rotational injuries 335
 correlated to strain in the brain as well as local brain 336
 motion experiments [28], [29]. 337

338 Another limitation with the test method presented here 338
 (and indeed with most helmet testing methods) is that 339
 only the head is used. A more realistic simulation would 340
 probably involve using the whole body, or at least the 341
 head, neck and torso. Involving for example the neck would 342
 change the dynamics of the impact, as the boundary 343
 conditions for the head would change. Ruan et. al. (1991) 344
 [30] showed that a single hinge coupling between the head 345
 and the neck had a limited effect on the intra-cranial 346

Table 2 Results from the numerical simulations.

Impact area*	Impact velocity	Impact angle	$\Delta\omega$ (rad/s)	FE model of the Hybrid III head			FE model of the human head
				HIC-value	Peak resultant translational acc (g)	Peak resultant rotational acc (krad/s ²)	Maximum strain in brain tissue
1	5	30	26.6	320	102	9.1	0.16
1	5	45	21.7	651	132	8.5	0.13
1	5	60	12.2	974	165	4.6	0.08
1	5	90	6.8	1183	191	2.6	0.10
1	7	30	35.6	652	145	11.8	0.23
1	7	45	26.5	1363	188	7.8	0.19
1	7	60	14.6	1939	217	4.9	0.11
1	7	90	9.5	2279	243	3.6	0.12
1	9	30	45.0	1083	177	14.2	0.30
1	9	45	34.4	2206	220	11.6	0.24
1	9	60	21.2	3178	264	9.2	0.14
1	9	90	12.3	3791	294	4.8	0.12
2	3	30	20.8	50	52	6.3	0.13
2	3	45	19.5	95	65	6.5	0.13
2	3	60	16.9	139	75	5.9	0.14
2	3	90	12.9	183	80	4.7	0.12
2	5	30	32.9	134	73	9.2	0.22
2	5	45	31.3	262	97	10.0	0.23
2	5	60	27.4	394	115	9.4	0.23
2	5	90	21.5	536	126	8.8	0.19
2	7	30	44.4	255	92	11.4	0.32
2	7	45	42.7	515	126	12.9	0.32
2	7	60	36.9	811	151	12.3	0.31
2	7	90	29.0	1252	165	11.6	0.25
2	9	30	54.1	384	109	13.4	0.40
2	9	45	52.8	883	152	16.1	0.43
2	9	60	46.3	1658	196	15.0	0.43
2	9	90	34.3	3152	280	13.4	0.34
3	5	30	25.2	318	100	7.4	0.12
3	5	45	16.6	614	133	8.4	0.14
3	5	60	7.3	827	157	2.9	0.15
3	5	90	15.3	922	171	5.6	0.19
3	7	30	33.7	664	134	9.9	0.18
3	7	45	22.3	1244	173	8.7	0.18
3	7	60	12.2	1670	195	6.8	0.20
3	7	90	20.0	1840	220	8.6	0.25
3	9	30	43.6	1094	162	12.0	0.24
3	9	45	30.4	2119	210	8.1	0.23
3	9	60	16.9	3010	239	9.8	0.27
3	9	90	24.8	3553	285	10.0	0.34

* Defined in figure 3

347 pressure during impact. Beusenberg et. al. (2001) [31]
 348 simulated the influence of different neck models using
 349 data from head impacts recorded from the National Football
 350 League in the US. In that study, it was shown that for
 351 oblique impacts to the front of the head, the coupling
 352 between the head and the neck is only important for
 353 rotations in the sagittal plane. These rotations are however

strongly dependent on the boundary conditions of the 354
 neck. Hering and Derler (2000) [32] performed both radial 355
 and oblique helmet impact tests on both a detached Hybrid 356
 III dummy head and a complete Hybrid III dummy. It 357
 could be concluded from their study, that the influence of 358
 the neck and body on the rotational effects in the head 359
 was different for different impact locations. They also 360

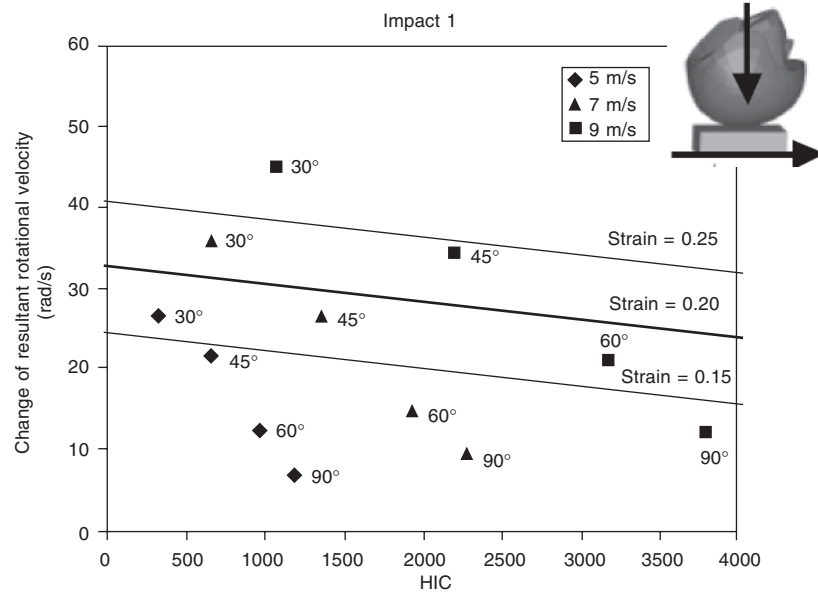


Figure 5 Results from impact 1, where the axes represents computed levels in the FE Hybrid III head model, and the straight lines are isostrain curves representing different strain levels in the brain tissue in the FE human head model.

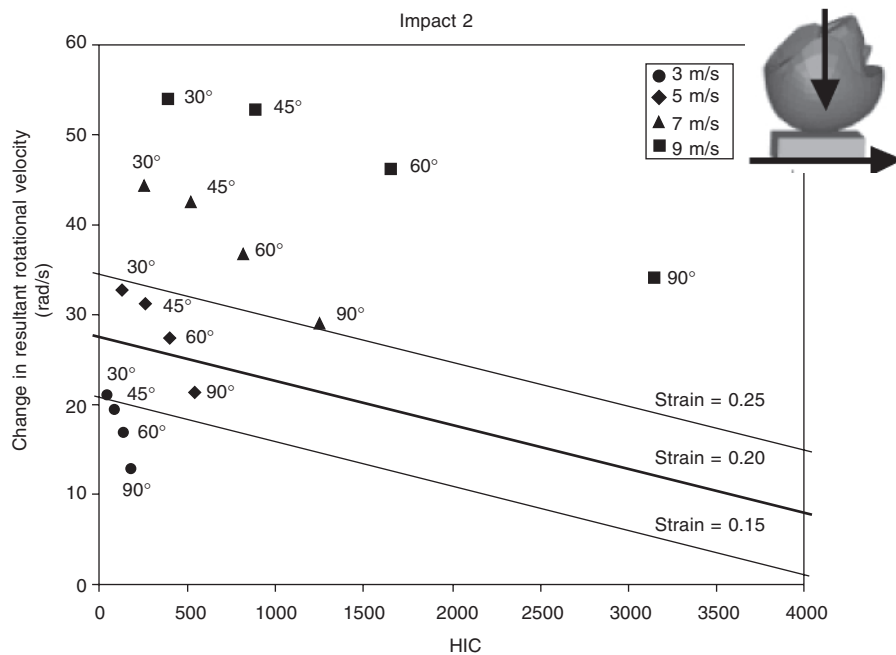


Figure 6 Results from impact 2, where the axes represents computed levels in the FE Hybrid III head model, and the straight lines are isostrain curves representing different strain levels in the brain tissue in the FE human head model.

361 concluded that because the Hybrid III neck is much stiffer
 362 than the human neck, this presented a problem. It is
 363 proposed here that the influence of the neck ought to be
 364 investigated in future studies.

365 **CONCLUSIONS**

366 When comparing the FE Hybrid III head model kinematics
 367 with strains in the FE human brain tissue during oblique

impacts, it can be concluded that rotational kinematics 368
 are as important as translational kinematics and should 369
 therefore be included in future head injury criteria. In 370
 Impact 1, changes in the rotational velocity provide a critical 371
 parameter. In Impact 2 and 3, changes in rotational velocity 372
 as well as the HIC value are important indicators (reiterating 373
 here, Impact 1 is to the top of the head inducing sagittal 374
 plane rotation, Impact 2 is lateral inducing axial rotation, 375
 and Impact 3 is lateral inducing coronal plane rotation). 376

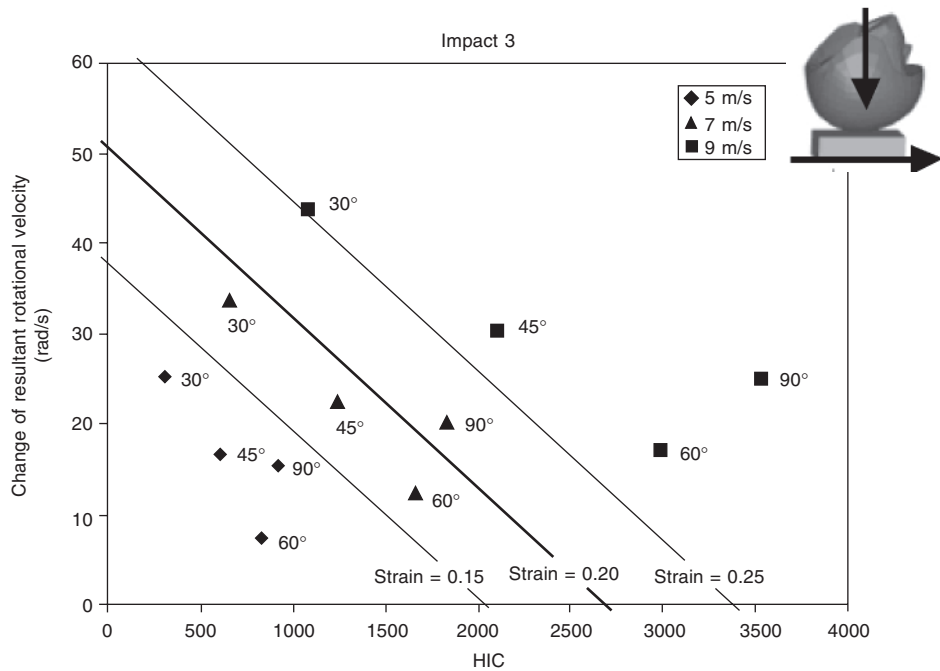


Figure 7 Results from impact 3, where the axes represents computed levels in the FE Hybrid III head model, and the straight lines are isostrain curves representing different strain levels in the brain tissue in the FE human head model.

Table 3 Constants k_1 and k_2 and the regression coefficient r^2 from the regressions analysis.

	Impact 1	Impact 2	Impact 3
k_1	$6.14 \cdot 10^{-3}$	$7.26 \cdot 10^{-3}$	$3.92 \cdot 10^{-3}$
k_2	$1.32 \cdot 10^{-5}$	$3.50 \cdot 10^{-5}$	$7.41 \cdot 10^{-5}$
r^2	0.93	0.97	0.68

377 This study shows that it is possible to make a good
 378 prediction of the strain in the brain tissue using the peak
 379 change of rotational velocity and the HIC value. Test-
 380 specific injury thresholds should therefore include both
 381 rotational and translational parameters, such as the change
 382 in rotational velocity and HIC. The results presented here
 383 can be helpful in preventing head injuries through their
 384 consideration in the setting of future standards for oblique
 385 impact helmet tests.

386 **ACKNOWLEDGEMENT**

387 The authors wish to thank the Länsförsäkringar
 388 Corporation Research Found and VINNOVA for financial
 389 support.

390 **REFERENCES**

391 1. AARE, M and VON HOLST, H. (2003). Injuries from
 392 Motorcycle- and Moped crashes in Sweden from 1987 to
 393 1999, Injury Control and Safety Promotion, vol. 10, No. 3,
 394 pp.131–138.

2. GENNARELLI, T A. (1983). Head Injury in Man and 395
 Experimental Animals: Clinical Aspects, Acta 396
 Neurochirurgica, Suppl. 32, pp. 1–13. 1983. 397
 3. OTTE, D, CHINN, B, DOYLE, D, MÄKITUPA, S, STURROCK, K 398
 and SCHULLER, E. (1999). Contribution to Final Report of 399
 COST 327 Project, University of Hanover. 400
 4. [ECE22.05] United Nations, Economic commission for 401
 Europe, working party WP29 on the Construction of 402
 Vehicles, Regulation 22, Uniform provisions concerning the 403
 approval of protective helmets for drivers and passengers of 404
 motorcycles and mopeds, Geneva, Initially passed 1958, 405
 amendment 03 1988, amendment 04 1995, amendment 05 406
 1999. 407
 5. [FMV218] Federal motor vehicle standard No 218, U.S. 408
 Government Printing Office, 1997. 409
 6. [BS6658] British Standards Institution. (1985). Protective 410
 helmets for vehicle users', BS 6658, London. 411
 7. AARE, M and HALLDIN, P. (2003). A New Laboratory Rig 412
 for Evaluating Helmets subject to Oblique Impacts, Traffic 413
 Injury Prevention, Vol. 4, Issue 3, pp. 240–248. 414
 8. MARGULIES, S S and THIBAUT, L E. (1992). A proposed 415
 Tolerance Criterion for Diffuse Axonal Injuries in Man. J. 416
 of Biomechanics, 25 (89), pp. 917–923. 417
 9. DiMASI, F P, EPPINGER, R H and BANDA, F A. (1995). 418
 Computational Analysis of Head Impact Response Under 419
 Car Crash Loadings. Proceedings to the 39th STAPP Car 420
 Crash Conference, San Diego, SAE 952718. 421
 9. DiMasi, F P, Eppinger, R H and BANDA, F A. (1995). 422
 Computational Analysis of Head Impact Response Under 423
 Car Crash Loadings. Proceedings to the 39th STAPP Car 424
 Crash Conference, San Diego, SAE 952718. 425
 10. UENO, K and MELVIN, J. (1995). Finite Element Model 426
 Study of Head Impact Based on Hybrid III Head 427
 Acceleration: The Effects of Rotational and Translational 428

- 429 Acceleration, *Journal of Biomechanical Engineering*, August
430 1995, vol. 117 pp. 319–328.
- 431 11. KLEIVEN, S and VON HOLST, H. (2003). Review and
432 evaluation of head injury criteria, *Proc. RTO Specialist*
433 *Meeting, the NATO, Coblenz, Germany*.
- 434 12. BAIN, B C and MEANEY, D F. (2000). Tissue-Level
435 Thresholds for Axonal Damage in an Experimental Model
436 of Central Nervous System White Matter Injury, *J.*
437 *Biomech. Eng.*, 16, pp. 615–622.
- 438 13. HOLBOURN, A H S. (1943). Mechanics of head injury,
439 *Lancet* 2, October 9, pp. 438–441.
- 440 14. HALLQUIST, J O. (1998). LS-DYNA3D Theoretical Manual.
441 Livermore Software Technology Corporation.
- 442 15. KLEIVEN, S. (2003). Influence of Impact Direction to the
443 Human Head in Prediction of Subdural Hematoma. *Journal*
444 *of Neurotrauma* 20 (4), pp. 365–379.
- 445 16. FREDRIKSSON, L A. (1996). A Finite Element Data Base for
446 Occupant Substitutes, Doctoral Thesis. Dissertations No.
447 447, Division of Solid Mechanics, Dept. of Mech.
448 Engineering, Linköping University, Sweden.
- 449 17. National Highway Traffic Safety Administration (NHTSA),
450 Department of Transportation (DOT), (1972). Occupant
451 Crash Protection – Head Injury Criterion S6.2 of MVSS
452 571.208, Docket 69-7, Notice 17. NHTSA, Washington,
453 DC.
- 454 18. Visible Human Project. Web site: www.nih.gov 14-08-2003.
- 455 19. KLEIVEN, S and VON HOLST, H. (2001). Consequences of
456 brain size following impact in prediction of subdural
457 hematoma evaluated with numerical techniques, in: *IRCOBI*
458 *Conference 2001, Isle of Man (UK)*, 161–172.
- 459 20. KLEIVEN, S and VON HOLST, H. (2002). Consequences of
460 head size following trauma to the human head. *Journal of*
461 *Biomechanics* 35 (2), 153–160, 2002.
- 462 21. KLEIVEN, S and HARDY, W N. (2002). Correlation of an FE
463 Model of the Human Head with Experiments on Localized
464 Motion of the Brain – Consequences for Injury Prediction.
465 SAE Paper No. 02S-76, Society of Automotive Engineers.
466 46th Stapp Car Crash Journal.
- 467 22. YETTRAM, A L, GODFREY, N P M and CHINN, B P. (1994).
468 Materials for motorcycle crash helmets – a finite element
469 parametric study, *Plastic, Rubber and Composites*
470 *Processing and Applications*, 22(1994) pp. 215–221
23. GENNARELLI, T A, THIBAUT, L E, ADAMS, J H. (1982).
471 Diffuse Axonal Injury and Traumatic Coma in the Primate,
472 *Ann. Neurol.* 12, pp. 564–574. 473
24. GENNARELLI, T A, THIBAUT, L E, TOMEI, G. (1987).
474 Directional dependence of axonal brain injury due to
475 centroidal and non-centroidal acceleration, SAE Paper No.
476 872197, Proc. 31st Stapp Car Crash Conference, Society of
477 Automotive Engineers, Warrendale, PA, pp. 49–53. 478
25. NEWMAN, J A, SHEWCHENKO, N and WELBOURNE, E. (2000).
479 A Proposed New Biomechanical Head Injury Assessment
480 Function – The Maximum Power Index, Proc. 44th Stapp
481 Car Crash Conf., SAE Paper No. 2000-01-SC16. 482
26. BAIN, B C, BILLIAR, A C, SHREIBER, D I, MCINTOSH, T K
483 and MEANEY, D F. (1996). In Vivo Mechanical Thresholds
484 for Traumatic Axonal Damage. AGARD AMP Specialists
485 Meeting on Impact Head Injury, New Mexico 7–9
486 November 1996. 487
27. DONNELLY, B R. (1998). Brain tissue material properties: A
488 comparison of results. Biomechanical research:
489 Experimental and computational, Proc. 26th Int. Workshop,
490 pp. 47–57. 491
28. HARDY, W N, FOSTER, C D, MASON, M J, YANG, K H, KING,
492 A I and TASHMAN, S. (2001). Investigation of Head Injury
493 Mechanisms Using Neutral Density Technology and High-
494 Speed Biplanar X-ray. SAE Paper No. 01S-52, in: 45th
495 Stapp Car Crash Conf., Society of Automotive Engineers,
496 pp. 337–368. 497
29. KING, A I, HARDY, W N, MASON, M J and TASHMAN, S.
498 (2002). Comparison of Relative Motion Between the Brain
499 and Skull of the Human Cadaver for Rotation in the
500 Coronal and Sagittal Planes, 4th World Congress of
501 Biomechanics. August 2002, Calgary, Alberta, Canada. 502
30. RUAN, J S, KHALIL, T and KING, A I. (1991). Human Head
503 Dynamic Response to Side Impact by Finite Element
504 Modeling, *J. Biomechanical engineering*, 113(3) pp. 276–283. 505
31. BEUSENBERG, M, SHEWCHENKO, N, NEWMAN, J A, DE LANGE,
506 R and CAPPON, H. (2001). In: *IRCOBI Conference 2001,*
507 *Isle of Man (UK)*, 295–310. 508
32. HERING, A M and DERLER, S. (2000). Motorcycle helmet
509 drop tests using a Hybrid III dummy, in: *IRCOBI*
510 *Conference, Montpellier, France, September 2000*, pp. 307–
511 321. 512